

## Electronic structure and Fermi surface of Ni<sub>3</sub>Fe

T. Nautiyal and S. Auluck

*Department of Physics, University of Roorkee, Roorkee 247 667, India*

(Received 30 July 1992; revised manuscript received 18 September 1992)

We have studied the electronic structure of the strongly ferromagnetic compound, ordered Ni<sub>3</sub>Fe. The calculations are done self-consistently using a semirelativistic linear-muffin-tin-orbital method in the atomic-sphere approximation. A basis of *s*, *p*, and *d* orbitals is used. Different Wigner-Seitz radii are used for Ni and Fe atoms. We present a detailed theoretical study of the Fermi surface of Ni<sub>3</sub>Fe. A comparison with the Fermi surface of Ni<sub>3</sub>Al, for which experimental data are also available, makes an interesting study and points to the consistency of our calculations.

### I. INTRODUCTION

Elements of the transition group are known to form alloys possessing solid solubility over extended regions of composition. One of the most widely used systems in industry is the transition-metal alloy system Ni-Fe. These alloys are useful in many technological applications due to their numerous interesting physical properties. Most significantly, these alloys exhibit invar behavior, which is a favorable circumstance since it keeps the thermal expansion rather low near room temperature. Such a low thermal expansion is often a requirement in modern magnetomotion constructions. A low thermal expansion may be required particularly in those cases where the permanent-magnet material is used in the form of a thin magnetic film.<sup>1</sup> Recently, Moroni and Jarlborg<sup>2</sup> have shown qualitatively that thermal excitations of the ferromagnetic ground state to the higher nonmagnetic state are able to produce typical invar properties in Fe<sub>3</sub>Ni. The energy difference between the two states is, according to the local-density results, small and comparable to the thermal energy  $k_B T$ . Also, due to sensitivity of the mechanical properties of these alloys to atomic ordering, they have been extensively studied experimentally. Recently, Podgórný<sup>3</sup> and Jepsen and Herman<sup>4</sup> presented a theoretical study of this alloy system. Some of the Ni-Fe alloys exist in ordered as well as in disordered form. One such alloy is Ni<sub>3</sub>Fe, which is known to have nearly the same atomic moments in ordered and disordered phases.<sup>5</sup> Neutron diffraction and magnetization experiments<sup>5,6</sup> on highly ordered Ni<sub>3</sub>Fe give  $\mu_{Fe} = 3.10(\pm 0.01)\mu_B$  and  $\mu_{Ni} = 0.682(\pm 0.005)\mu_B$ . The ordering temperature of this alloy is estimated to be 490°C by Shull and Wilkinson,<sup>5</sup> 503°C by Cranshaw,<sup>7</sup> and  $\approx 547^\circ\text{C}$  by Orehtsky, Sousa, and Pinheiro.<sup>8</sup>

Ordered Ni<sub>3</sub>Fe crystallizes in the Cu<sub>3</sub>Au crystal structure. Earlier work on this alloy has been summarized efficiently in the work of Podgórný.<sup>3</sup> He has calculated ground-state properties, such as equilibrium lattice constants, state equations, average and local magnetic moments and their volume dependence, and cohesive properties of Ni-Fe alloys, using the semirelativistic linear-muffin-tin-orbital (LMTO) method. In his work, the cal-

culations are done at an average Wigner-Seitz (WS) radius of 2.624 a.u. for all the compounds and the ratio of atomic spheres  $S_{Fe}/S_{Ni}$  has been taken as 1.027, the value obtained from the ratio of atomic volumes of elemental Fe and Ni in their ground states. Jepsen and Herman<sup>4</sup> have concentrated on understanding the magnetic properties of the permalloy-Mn-Fe alloy interface on an atomic scale, hence they have studied 15 ordered compounds, such as binary Fe-Ni and Mn-Fe alloys and ternary Mn-Fe-Ni alloys, defined by the formula  $Mn_m Fe_n Ni_{4-m-n}$ , where *m* and *n* are integers with  $0 \leq m, n \leq 4$ . The method used is the self-consistent LMTO method and the same WS radii have been used at the two atomic sites. They<sup>4</sup> describe the dependence of the atomic moments on the composition and lattice constants over the entire composition range of this system. Hence, their work gives only the atomic moments for Ni<sub>3</sub>Fe. However, some of their results on Ni<sub>3</sub>Fe may be found in the work of Frota-Pessôa,<sup>9</sup> where these results are compared with those obtained from spin-polarized bands via the recursion method. Thus, although the Ni-Fe system as a whole has been studied in great details, Ni<sub>3</sub>Fe has not been studied as exhaustively. This is one of the reasons why we embarked on such a study. Also, recently, we made a detailed study<sup>10</sup> of the Fermi surface of weakly ferromagnetic Ni<sub>3</sub>Al, which also crystallizes in the Cu<sub>3</sub>Au structure, and obtained good agreement with the experimental data. Ni<sub>3</sub>Fe, being strongly ferromagnetic, is expected to have a much larger exchange splitting between the majority- and minority-carrier bands, as compared to the case of Ni<sub>3</sub>Al. Thus it would be even more interesting, and at the same time, a challenging task to study the Fermi surface of Ni<sub>3</sub>Fe, which may have more structure and which, to our knowledge, as yet has not been studied, either theoretically or experimentally. Hence, this work provides a detailed study of the electronic structure, as well as the Fermi surface of Ni<sub>3</sub>Fe. We hope that our work will encourage some dHvA measurements on this alloy.

The plan of the paper is as follows: we briefly describe the method used in Sec. II; results and discussions constitute Sec. III, and conclusions of this study are summed up in Sec. IV.

## II. METHOD OF CALCULATION

A self-consistent LMTO method, based on the atomic-sphere approximation with combined correction terms,<sup>11,12</sup> has been used here. The calculations are semirelativistic in nature. The exchange-correlation (XC) potential used is the Barth-Hedin potential.<sup>13</sup> It is assumed that the core charge remains unchanged in the process of formation of solid from free atoms. Therefore, atomic charge densities are used throughout the calculations. The wave function is expanded in *s*, *p*, and *d* orbitals at each atomic site. The experimental lattice constant<sup>14</sup> for Ni<sub>3</sub>Fe is 3.55 Å, which corresponds to an average WS radius of 2.624 a.u. Our calculations are performed using this value. We have used different WS radii for the Ni and Fe atomic spheres, following the method outlined by Andersen, Jepsen, and Sob,<sup>15</sup> which has been used for Pd<sub>3</sub>Fe by Bose *et al.*,<sup>16</sup> and for Ni<sub>3</sub>Al in our previous paper.<sup>10</sup> The ratio of the radii of the atomic spheres  $S_{\text{Fe}}/S_{\text{Ni}}$  is equal to 1.023. The one-electron potentials were self-consistently obtained using 84k points in the irreducible Brillouin zone. This number of *k* points has been taken as smaller than the 220k points used for Ni<sub>3</sub>Al, see Ref. 10, because the error introduced is very small and a great deal of computer time is saved. We have used the tetrahedron method<sup>17</sup> to calculate the density of states (DOS).

## III. RESULTS AND DISCUSSION

Our calculations are performed at an experimental WS radius of 2.624 a.u., which is very close to the value of 2.62 a.u. used by Podgórný.<sup>3</sup> Also, the ratio of  $S_{\text{Fe}}/S_{\text{Ni}}$  for our work (1.023) is very close to 1.027, used by Podgórný.<sup>3</sup> However, in Ref. 3, the local XC potential is parametrized according to Vosko, Wilk, and Nusair.<sup>18</sup> It is our experience<sup>19</sup> that the use of different XC parametrizations usually leads to slightly different results. Hence, the use of different XC potentials is expected to be the main factor for any differences in our results and those from Ref. 3. On the other hand, Jepsen and Herman<sup>4</sup> have also used Barth-Hedin XC potentials, but have chosen the same WS radii at the two atomic sites.

Therefore, the latter factor may lead to differences between our results and theirs.<sup>4</sup> We first discuss the nonmagnetic phase of Ni<sub>3</sub>Fe, which is the starting point in our calculations for the ferromagnetic phase.

### A. Nonmagnetic Ni<sub>3</sub>Fe

The important band parameters are given in Table I. Our band widths are in good agreement with those of Podgórný<sup>3</sup> (also given in Table I). Figure 1 displays the *d*-DOS at the two atomic sites for nonmagnetic Ni<sub>3</sub>Fe. The total DOS at the two atomic sites for nonmagnetic Ni<sub>3</sub>Fe is shown in Fig. 2. A comparison of the two figures shows that most of the contributions at and near the Fermi energy  $E_F$  comes from the Fe-*d* states. Also, the contribution from the *d* states to the total DOS at the two sites is predominant. Below  $E_F$ , there is a greater contribution from the Ni-*d* states than from the Fe-*d* states. The contribution from the *s* states, especially from the Ni-*s* states, is substantial only at very low energies of 0.25–0.35 Ry. The band structure of nonmagnetic Ni<sub>3</sub>Fe has flat bands for certain *k* regions, which correspond to peaks in the Fe-DOS curve. Thus, these are Fe-*d* bands. Our DOS curve in Fig. 1 agrees very well, qualitatively as well as quantitatively, with that of Podgórný.<sup>3</sup> The total DOS,  $N(E_F)$ , at Fermi energy is 139.85 states/Ry unit cell. Using the expression  $\gamma = (1/3)\pi^2 k_B^2 N(E_F)$  for the coefficient of electronic specific heat  $\gamma$ , we obtain  $\gamma$  equal to 24.26 mJ/mol K<sup>2</sup>, which is very large compared to the experimental value<sup>20</sup> of 13.2 mJ/mol K<sup>2</sup> for ferromagnetic Ni<sub>3</sub>Fe. The large value of  $N(E_F)$  shows that this nonmagnetic state is unstable for the formation of a ferromagnetic state, since the Stoner criterion for magnetism  $IN(E_F) > 1$  is satisfied. The Stoner parameter *I* for transition metals and their compounds may be written as<sup>21</sup>

$$I = \sum_t I_t [N_t(E_F)/N(E_F)]^2,$$

where  $I_t$  is the Stoner parameter for *d* orbitals at site *t* and  $N_t(E_F)$  is the *d*-DOS at site *t*. For  $I_t$  we have used the values from the work of Janak.<sup>22</sup>

TABLE I.  $\mu$  is the effective *d*-band mass at site *t* (in units of free-electron mass),  $A - B$  is the self-consistently calculated *d* bandwidth at site *t* (in mRy),  $W$  is the *d* bandwidth estimated on the basis of canonical band theory (in mRy),  $\eta = (A - B)/W$ , and  $\bar{\eta}$ -ideal ratio (see Ref. 3 for details).

Site	$\mu$		$A - B$		$W$		$\eta$		$\bar{\eta}$
	a	b	a	b	a	b	a	b	
Nonmagnetic Ni <sub>3</sub> Fe									
Ni	12.52	12.37	287	292	216	219	1.33	1.33	1.21
Fe	9.88	9.84	343	344	47	47	7.30	7.32	7.92
Ferromagnetic Ni <sub>3</sub> Fe									
Ni ↑	12.16		295		222		1.33		
↓	12.07		297		224		1.33		1.21
Fe ↑	10.63		318		44		7.23		
↓	9.55		354		49		7.22		7.92

<sup>a</sup>This work.

<sup>b</sup>Reference 3.

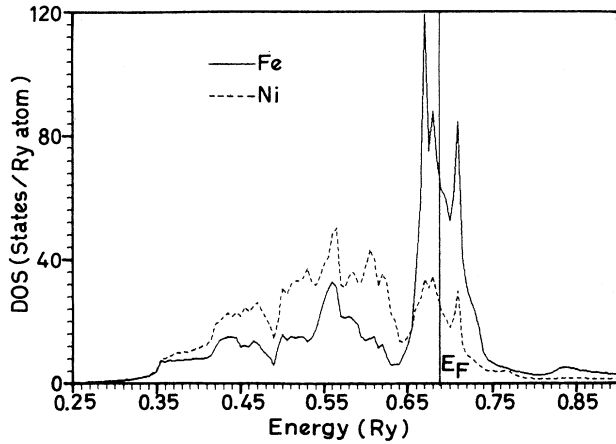


FIG. 1. *d*-band density of states for nonmagnetic  $\text{Ni}_3\text{Fe}$ . The solid curve is for the Ni site and the broken curve for the Fe site.

## B. Ferromagnetic state

### 1. Electronic structure

A comparison of the band structure of majority and minority carriers (not displayed here) shows that there is a large splitting of the spin-up and spin-down bands, which in itself is suggestive of this compound being a strong ferromagnet. The important band parameters for ferromagnetic  $\text{Ni}_3\text{Fe}$  are given in Table I. We find that spin-down bands are wider, compared with spin-up bands, for Fe-*d* states.

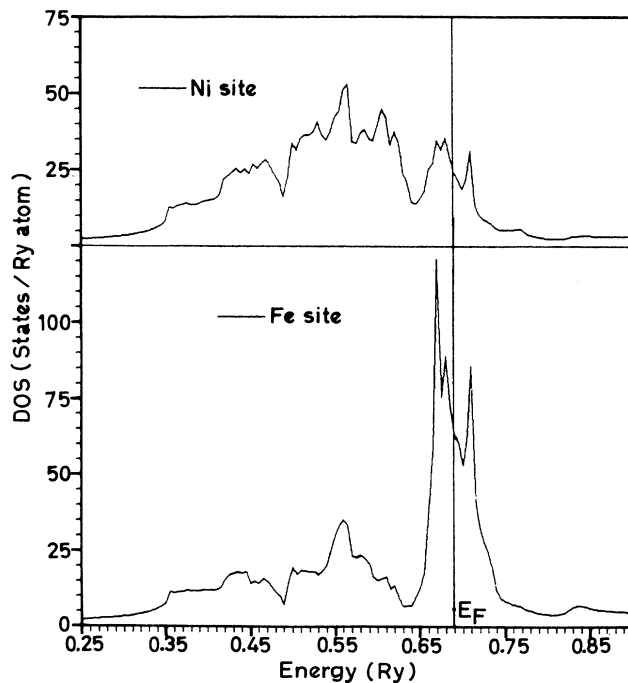


FIG. 2. Total DOS at the two atomic sites in nonmagnetic  $\text{Ni}_3\text{Fe}$ .

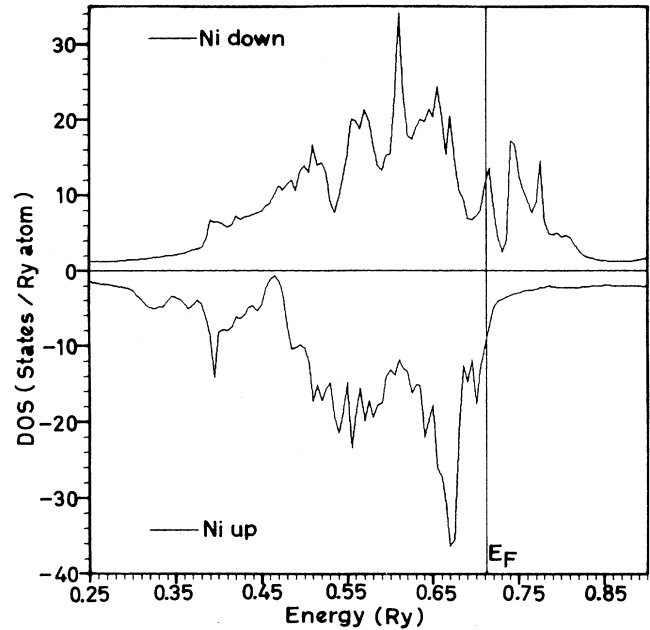


FIG. 3. The majority- and minority-carrier density of states at the Ni site.

The total DOS for majority and minority carriers at Ni site (Fe site) is shown in Figs. 3 and 4, respectively. The Fermi level is located slightly above the majority-carrier DOS, hence most of the spin-up states are filled for both types of atoms, while the pronounced peak for Fe spin-down bands corresponds to vacant states. The Ni and Fe spin-up electrons, therefore, form a common *d* band, while the spin-down electrons in Fe are almost excluded

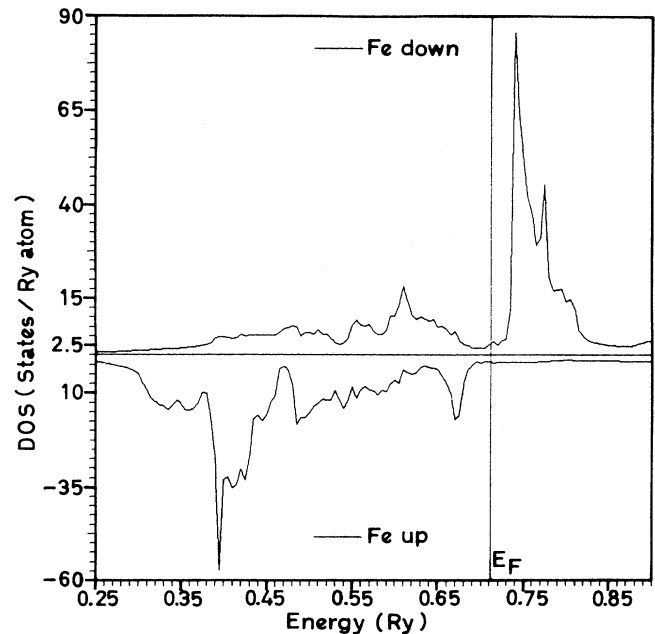


FIG. 4. Same as Fig. 3, but at the Fe site.

from the Fe site, producing a localized magnetic moment. The same picture is found for the Fe spin-down states in the case of Pd<sub>3</sub>Fe also.<sup>23</sup> However, unlike Pd<sub>3</sub>Fe, the DOS curves for Fe spin-up and spin-down states are quite different in shape and cannot be explained by a rigid shifting of the spin-up and spin-down bands when switching on the exchange interaction. A comparison of Figs. 3 and 4 with Figs. 3(b) and 3(d), of Ref. 9, respectively, for LMTO calculations of Jepsen and Herman<sup>4</sup> shows good agreement. The exchange splitting of spin-up and spin-down bands has resulted in a sharp drop of total DOS at Fermi energy  $N(E_F)$  to 41.55 states/Ry unit cell, which is close to the value<sup>24</sup> obtained by Jepsen and Herman.<sup>4</sup> The corresponding coefficient of electronic specific heat  $\gamma$  is 7.21 mJ/mol K.<sup>2</sup> This is much reduced compared to 24.26 mJ/mol K<sup>2</sup> for the nonmagnetic case and has become about half the experimental value<sup>20</sup> of 13.2 mJ/mol K.<sup>2</sup> This gives the renormalization parameter  $\lambda$  equal to 0.83, which indicates that this is a highly renormalized system. A comparison of total DOS from three Ni atoms and the Fe atom in a unit cell, shows that the maximum contribution from Fe states comes from a small energy range near 0.4 and 0.77 Ry, where it is comparable to the Ni contribution. For the rest of the energies, the DOS of Ni is dominant. Except for very low energies (0.25–0.30 Ry), where the Ni-*s* up and down DOS dominates, Ni-*d*-DOS and Fe-*d*-DOS are the chief contributors to the DOS curve. The various contributions to the DOS at  $E_F$  are given in Table II.

The partial charge occupancies for Ni and Fe are given in Table II. The exchange splitting of spin-up and spin-down bands gives rise to a total magnetic moment of 4.40  $\mu_B$  per unit cell or an average value of 1.10  $\mu_B$  per atom. We obtain the magnetic moment at the Fe sites as 3.12  $\mu_B$ /atom and at the Ni site, it is 0.43  $\mu_B$ /atom. A

comparison with the experimental value<sup>5</sup> and other theoretical values<sup>3,4</sup> listed in Table II shows that our  $\mu_{Fe}$  is in excellent agreement with the experimental value of 3.10( $\pm 0.01$ )  $\mu_B$ /atom while Refs. 3 and 4 underestimate it. However, the magnetic moment at the Ni site is underestimated by all theoretical works (Podgórný<sup>3</sup> has not reported the value at the Ni site). The difference in our magnetic moment values and those from Refs. 3 and 4 may be explained as follows: Podgórný<sup>3</sup> used a different XC potential, which should be the main factor responsible for the difference, as mentioned in the beginning of Sec. III. Jepsen and Herman<sup>4</sup> used the same WS radii at the two atomic sites, which certainly gives slightly different magnetic moments.<sup>10,19</sup> Besides this, a small difference in the results may be due to the use of different convergence criteria and the number of  $\mathbf{k}$  points.

One can write the Stoner criterion as<sup>25</sup>

$$\Delta E = mI ,$$

for both atomic species, where  $\Delta E$  is the split between the center of the up and down *d* bands for an atomic site,  $m$  is the corresponding *d*-band magnetization, and  $I$  is the Stoner parameter for the same site. Using  $I_{Fe} = 0.066$  Ry and  $I_{Ni} = 0.072$  Ry (Ref. 22) and our  $m_{Fe} = 3.00 \mu_B$ /atom and  $m_{Ni} = 0.46 \mu_B$ /atom for *d* bands, we obtain  $\Delta E_{Fe} = 0.20$  Ry and  $\Delta E_{Ni} = 0.03$  Ry. Our self-consistent band-structure calculations give<sup>12</sup>  $\Delta E = C_{\uparrow} - C_{\downarrow}$  (where  $C$  is the center of the respective *d* band), equal to 0.24 Ry and 0.02 Ry for Fe and Ni *d* bands, respectively. These values are quite close to  $\Delta E$  from Stoner criteria. This reflects the consistency of our band-structure calculation.

We have calculated the total energies  $E$  of Ni<sub>3</sub>Fe for the nonmagnetic (NM) and ferromagnetic (FM) phases at the experimental WS radius 2.624 a.u. used in this work.

TABLE II. *l*-projected density of states at the Fermi energy, in states/Ry unit cell, coefficient of electronic specific heat  $\gamma$ , in mJ/mol K<sup>2</sup>, charge occupancies, in electrons, and magnetic moment, in  $\mu_B$ , at the two atomic sites in Ni<sub>3</sub>Fe.

	Ni- <i>s</i>	Ni- <i>p</i>	Ni- <i>d</i>	$\mu_{Ni}$	Fe- <i>s</i>	Fe- <i>p</i>	Fe- <i>d</i>	$\mu_{Fe}$	Total	$\gamma$
<i>l</i> -projected DOS										
Nonmagnetic	0.20	0.84	23.99		0.20	1.14	63.40		139.86	24.26
Ferromagnetic $\uparrow$	0.19	0.45	4.72		0.18	0.30	1.45		18.03	
$\downarrow$	0.01	0.16	6.67		0.02	0.08	2.88		23.52	7.21
Experiment <sup>a</sup>										13.2
Charge occupancies										
Nonmagnetic	0.67	0.77	8.60		0.62	0.73	6.55		38.00	
Ferromagnetic $\uparrow$	0.33	0.39	4.53		0.34	0.44	4.67		21.19	
$\downarrow$	0.34	0.41	4.07		0.30	0.36	1.67		16.79	
Mag. moment										
Theory <sup>b</sup>	-0.01	-0.02	0.46	0.43	0.04	0.08	3.00	3.12	4.40	
Theory <sup>c</sup>				0.57				2.88	4.59	
Theory <sup>c</sup>								2.86		
Experiment <sup>d</sup>				0.682				3.10		
				( $\pm 0.005$ )				( $\pm 0.01$ )		

<sup>a</sup>Reference 21.

<sup>b</sup>Reference 4.

<sup>c</sup>Reference 3.

<sup>d</sup>Reference 5.

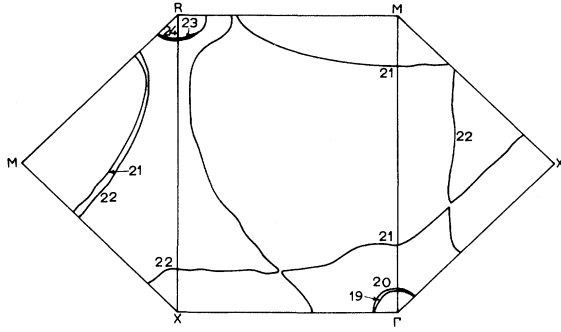


FIG. 5. Majority-carrier Fermi surface for ferromagnetic  $\text{Ni}_3\text{Fe}$ .

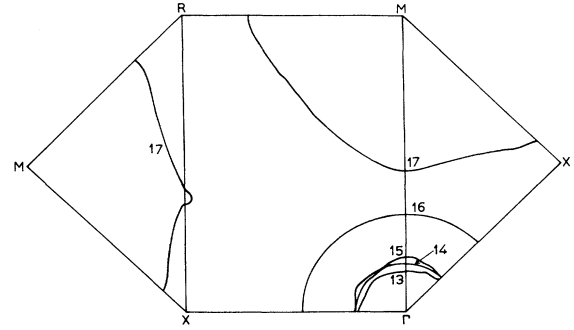


FIG. 6. Minority-carrier Fermi surface for ferromagnetic  $\text{Ni}_3\text{Fe}$ .

Our calculations yield  $E(\text{NM}) = -284.5413$  Ry and  $E(\text{FM}) = -284.5564$  Ry, giving  $E(\text{FM}) < E(\text{NM})$ , thus making it certain that  $\text{Ni}_3\text{Fe}$  is ferromagnetic. Our calculations give  $\Delta E = E(\text{NM}) - E(\text{FM}) = 15$  mRy or 3.8 mRy/atom. Since no other calculations are available, we compare this with  $\Delta E = 0.5$  mRy/atom for  $\text{Fe}_3\text{Ni}$  and 7 mRy/atom for Ni-Fe.

## 2. Fermi surface

Figures 5 and 6 display the Fermi surface (FS) cross sections for majority and minority carriers, respectively. We have used Stark's area-mass routine<sup>26</sup> to calculate the FS orbital areas and masses. For majority carriers, six (19th to 24th) bands cross the Fermi level, while for minority carriers, five (13th to 17th) bands do so. Due to

the large exchange splitting, none of the bands is common to the majority and minority FS's. Hence the two Fermi surfaces are entirely different and have no common features. The calculated orbit areas and effective band masses are given in Table III for most of the orbits.

Comparison of the majority-carrier FS with the majority-carrier FS of  $\text{Ni}_3\text{Al}$  (Ref. 10) interestingly shows many similarities (even though the bands responsible for this bear different indices). The majority-carrier FS for both  $\text{Ni}_3\text{Al}$  (14th and 15th bands) and  $\text{Ni}_3\text{Fe}$  (18th and 19th bands) have two small quasidegenerate  $\Gamma$ -centered hole pockets. Both have another medium-size  $\Gamma$ -centered hole pocket of similar shape (from the 16th band in  $\text{Ni}_3\text{Al}$  and from the 20th band in  $\text{Ni}_3\text{Fe}$ ). The size of  $\Gamma(110)$  open-hole orbit from the 17th band in  $\text{Ni}_3\text{Al}$  is so much increased in  $\text{Ni}_3\text{Fe}$  (from the 22nd band) that instead of cutting along  $\Gamma M$ , it is pinched off along  $RM$ . The corre-

TABLE III. Fermi surface orbit areas, in MG, and effective band masses, in free-electron units, for majority and minority carriers in  $\text{Ni}_3\text{Fe}$ .

Majority carriers			Minority carriers		
Orbit	Area	Mass	Orbit	Area	Mass
$\Gamma 19(100)$	2.72	-0.48	$\Gamma 13(100)$	10.50	-1.67
$\Gamma 19(110)$	2.76	-0.48	$\Gamma 13(110)$	10.61	-1.83
$\Gamma 19(111)$	2.65	-0.48	$\Gamma 13(111)$	10.01	-1.66
$\Gamma 20(100)$	3.11	-0.60	$\Gamma 14(100)$	13.91	-0.57
$\Gamma 20(110)$	3.03	-0.56	$\Gamma 14(110)$	13.75	-0.57
$\Gamma 20(111)$	3.20	-0.66	$\Gamma 14(111)$	14.12	-0.64
$\Gamma 21(100)$	45.91	-4.92	$\Gamma 15(100)$	15.57	-1.56
$\Gamma 21(110)$	40.22	-6.34	$\Gamma 15(110)$	14.99	-1.15
$\Gamma 21(111)$	32.18	-6.57	$\Gamma 15(111)$	16.44	-1.62
$M 21(100)$	19.33	-0.66	$\Gamma 16(100)$	56.69	-0.69
$M 21(110)$	43.07	-1.03	$\Gamma 16(110)$	56.27	-0.73
$M 21(001)$	60.33	-1.67	$\Gamma 16(111)$	55.96	-0.84
$M 21(111)$	24.90	-0.81			
$M 22(001)$	67.41	-1.49	$M 17(100)$	148.86	4.96
$X 22(001)$	9.90	-1.68	$M 17(110)$	110.34	4.09
$XM 22(100)$	17.23	1.60	$X 17(001)$	20.35	-7.42
$R 23(001)$	4.01	0.34	$R 17(001)$	56.90	-4.15
$R 23(110)$	4.00	0.34	$RX 17(110)$	2.72	4.33
$R 23(111)$	4.00	0.35			
$R 24(001)$	3.71	0.32			
$R 24(110)$	3.66	0.31			
$R 24(111)$	3.47	0.31			

sponding  $X$ -centered hole necks in the (001) plane, however, remain unaffected by this enlargement. Both these compounds have two small quasidegenerate electron pockets centered at  $R$  (from the 18th and 19th spin-up bands in Ni<sub>3</sub>Al, and from the 23rd and 24th spin-up bands in Ni<sub>3</sub>Fe). There is some additional structure in majority-carrier FS of Ni<sub>3</sub>Fe, which may be attributed to a larger exchange splitting in this compound.

The minority-carrier FS in Fig. 6 has many features in common with Ni<sub>3</sub>Al (Ref. 10). The  $\Gamma_{13}$  (there is no experimental evidence for this orbit in Ni<sub>3</sub>Al),  $\Gamma_{14}$ ,  $\Gamma_{15}$ , and  $\Gamma_{16}$  hole pockets are present in the minority-carrier FS of Ni<sub>3</sub>Al also,  $\Gamma_{14}$  and  $\Gamma_{15}$  being quasidegenerate in both compounds. The 16th orbit, however, has no kinks in Ni<sub>3</sub>Fe (unlike Ni<sub>3</sub>Al), as the 17th band sheets do not approach it, and thus has a spherical shape. The 17th band FS sheet has a similar shape for both compounds in the (001) plane, but the neck with center along  $RX$  has a much smaller size in Ni<sub>3</sub>Fe. These similarities of majority- and minority-carrier FS sheets for Ni<sub>3</sub>Fe with those for Ni<sub>3</sub>Al may also be taken as a reassuring feature of our present work, since for Ni<sub>3</sub>Al, we had obtained a good agreement with experimental FS data.

#### IV. CONCLUSIONS

We have presented a detailed study of the electronic structure and the Fermi surface of ordered Ni<sub>3</sub>Fe. Different WS radii were used at the Ni and Fe sites, using the prescription of Andersen, Jepsen, and Sob.<sup>15</sup> We presented a comparison of our results with earlier LMTO calculations of Podgórny,<sup>3</sup> where the ratio of WS radii,  $S_{Fe}/S_{Ni}$ , is almost the same as in our work but a different

XC potential is used, and of Jepsen and Herman,<sup>4</sup> where the same XC potential is employed, but  $S_{Fe}/S_{Ni}$  is chosen as unity. Good overall agreement with available results is obtained. However, none of previous calculations<sup>3,4</sup> give much detail about spin-polarized Ni<sub>3</sub>Fe. Comparison of magnetic moments at Fe and Ni sites with experiment shows that we obtain much better values for  $\mu_{Fe}$ , which is underestimated in Refs. 3 and 4. The magnetic moment at the Ni site is, however, underestimated by this work as well as Ref. 4, while the value is not reported in Ref. 3.

We have presented a detailed calculation of the Fermi surface extremal orbit areas of Ni<sub>3</sub>Fe. Nonavailability of experimental and theoretical results prohibits any comparison. However, a comparison with the Fermi surface of weakly ferromagnetic Ni<sub>3</sub>Al, for which experimental as well as theoretical results are available, shows a number of similarities which point to the consistency of the present calculation. We hope our work would encourage the experimentalists to make Fermi surface measurements on Ni<sub>3</sub>Fe and help them in designing the setup on the basis of the Fermi surface areas/frequencies presented here.

#### ACKNOWLEDGMENTS

Financial support from the Council of Scientific and Industrial Research (CSIR), India, vide Scheme No. 3(698)/91-EMR-II is gratefully acknowledged. One of the authors (TN) wants to thank Professor Marek Podgórny for making available a number of his valuable reprints.

- <sup>1</sup>F. J. Cadieu, T. D. Cheung, and L. Wickramasekara, *J. Magn. Mater.* **54-57**, 535 (1986); F. J. Cadieu, T. D. Cheung, L. Wickramasekara, and N. Kamprath, *IEEE Trans. Magn. MAG-22*, 752 (1986); J. F. Zasadzinski, C. U. Segre, and E. D. Rippert, *J. Appl. Phys.* **61**, 4278 (1987).
- <sup>2</sup>E. G. Moroni and T. Jarlborg, *Physica B* **161**, 115 (1989).
- <sup>3</sup>M. Podgórny, *Acta Phys. Pol. A* **78**, 941 (1990).
- <sup>4</sup>O. Jepsen and F. Herman, *Phys. Rev. B* **41**, 6801 (1990).
- <sup>5</sup>C. G. Shull and M. K. Wilkinson, *Phys. Rev.* **97**, 304 (1955).
- <sup>6</sup>J. W. Cable and E. O. Wollan, *Phys. Rev. B* **7**, 2005 (1973).
- <sup>7</sup>T. E. Cranshaw, *J. Phys. F* **17**, 967 (1987).
- <sup>8</sup>J. Orehtsky, J. B. Sousa, and M. F. Pinheiro, *J. Appl. Phys.* **53**, 7939 (1982).
- <sup>9</sup>S. Frota-Pessôa, *Phys. Rev. B* **36**, 904 (1987).
- <sup>10</sup>T. Nautiyal and S. Auluck, *Phys. Rev. B* **45**, 13930 (1992).
- <sup>11</sup>O. K. Andersen, *Phys. Rev. B* **12**, 3060 (1975).
- <sup>12</sup>H. L. Skriver, *The LMTO Method: Muffin-Tin-Orbitals and Electronic Structure* (Springer, New York, 1984).
- <sup>13</sup>U. von Barth and L. Hedin, *J. Phys. C* **5**, 1629 (1972).
- <sup>14</sup>W. B. Pearson, *Handbook of Lattice Spacings and Structure of Metals* (Pergamon, Oxford, 1967), Vol. 2.
- <sup>15</sup>O. K. Andersen, O. Jepsen, and M. Sob, in *Electronic Band Structure and its Applications*, edited by M. Yussouff Springer-Verlag Lecture Notes in Physics Vol. 283 (Springer, Berlin, 1987).
- <sup>16</sup>S. K. Bose, J. Kudrnovsky, M. van Schilfgaarde, P. Blöchl, O. Jepsen, M. Methfessel, A. T. Paxton, and O. K. Andersen, *J.*

- Magn. Mater.* **87**, 97 (1990).
- <sup>17</sup>O. Jepsen and O. K. Andersen, *Solid State Commun.* **9**, 1763 (1971); G. Lehmann and M. Taut, *Phys. Status Solidi B* **54**, 469 (1972).
- <sup>18</sup>S. H. Vosko, L. Wilk, and M. Nusair, *Can. J. Phys.* **58**, 1200 (1983).
- <sup>19</sup>R. Ahuja, A. K. Solanki, and S. Auluck, *Phys. Status Solidi B* **168**, 509 (1991); A. K. Solanki, R. Ahuja, and S. Auluck, *Pramana* **38**, 189 (1992).
- <sup>20</sup>R. Kuentzler, *Phys. Status Solidi B* **58**, 519 (1973); R. Kuentzler and R. W. Waterstrat, in *Proceedings of the 17th International Conference on Low Temperature Physics, LT-17*, edited by U. Eckern, A. Schmid, W. Weber, and H. Wühl (Elsevier Science, BV, 1984).
- <sup>21</sup>S. S. Jaswal, *Solid State Commun.* **52**, 127 (1984).
- <sup>22</sup>J. F. Janak, *Phys. Rev. B* **16**, 255 (1977); O. K. Andersen, O. Jepsen, and D. Glötzel, in *Highlights of Condensed-Matter Theory*, edited by F. Bassani, F. Fumi, and M. P. Tosi (North-Holland, Amsterdam, 1985).
- <sup>23</sup>C. A. Kuhnen and E. Z. da Silva, *Phys. Rev. B* **35**, 370 (1985); T. Nautiyal and S. Auluck (unpublished).
- <sup>24</sup>The approximate value of DOS is 42 states/(Ry unit cell) as read from Figs. 3(b) and 3(d) of Ref. 9.
- <sup>25</sup>U. K. Poulsen, J. Kollar, and O. K. Andersen, *J. Phys. F* **6**, L241 (1976).
- <sup>26</sup>R. W. Stark (private communication).